Talanta 128 (2014) 215–220

Contents lists available at ScienceDirect

Talanta

journal homepage: www.elsevier.com/locate/talanta

Glutathione and L-cysteine modified silver nanoplates-based colorimetric assay for a simple, fast, sensitive and selective determination of nickel

Thanyaporn Kiatkumjorn [a,c], Poomrat Rattanarat [a], Weena Siangproh [b], Orawon Chailapakul [a,c], Narong Praphairaksit [a,*]

[a] Electrochemistry and Optical Spectroscopy Research Unit (EOSRU), Department of Chemistry, Faculty of Science, Chulalongkorn University, 254 Phayathai Road, Patumwan, Bangkok 10330, Thailand
[b] Department of Chemistry, Faculty of Science, Srinakharinwirot University, Sukhumvit 23, Wattana, Bangkok 10110, Thailand
[c] Center of Excellence on Petrochemical and Materials Technology, Chulalongkorn University, Patumwan, Bangkok 10330, Thailand

ARTICLE INFO

Article history:
Received 18 February 2014
Received in revised form
25 April 2014
Accepted 29 April 2014
Available online 9 May 2014

Keywords:
Colorimetric assay
Nickel ion
Silver nanoplates
Glutathione
L-cysteine

ABSTRACT

A novel colorimetric assay based on silver nanoplates (AgNPls) for detecting nickel ions (Ni^{2+}) has been developed. Glutathione (GSH) and L-cysteine (Cys) were used to modify the AgNPls surface, exhibiting extremely high selectivity towards Ni^{2+} over other metal ions under specific conditions. Upon addition of Ni^{2+} to the modified AgNPls solution, a distinctive color change can be clearly observed by naked eyes as a result of the aggregation of AgNPls induced by the binding between Ni^{2+} and the modified ligands. To verify a complete self-assembly of the GSH and Cys onto AgNPls surface, the modified AgNPls were characterized using Fourier transform infrared spectroscopy (FTIR), ultraviolet–visible spectroscopy (UV–vis) and transmission electron microscopy (TEM), respectively. Moreover, various parameters affecting the Ni^{2+} quantification including the modifier ratio, pH, reaction time, and interferences were investigated. With UV–vis spectrophotometric measurement under optimal conditions, a quantitative linearity was established in the range of 10–150 ppb (R^2=0.9971) with the detection limit of 7.02 ppb or 120 nM (S/N=3). In addition, the developed sensor was applied to the determination of Ni^{2+} in waste samples from a jewelry factory and a car manufacturer with satisfactory results. Overall, this alternative approach presents a simple, rapid, sensitive and selective detection of Ni^{2+}.

© 2014 Elsevier B.V. All rights reserved.

1. Introduction

The release of heavy metals into the environmental system is a critical worldwide issue due to the numerous number of toxic side effects associated with these metals [1]. In particular, nickel is a metallic element which has been widely used in various industries such as coins and jewelry manufacturing, battery production, and electroplating engineering. Once human exposes to nickel residue without knowing, potential risks of serious disorders including malignant tumors, nasopharynx, lung, and dermatological abnormality are relatively increased [2]. In order to evaluate the quality control of environmental monitoring, the maximum limits of nickel in water have been established by the World Health Organization (WHO) and the United States Environmental Protection Agency (EPA) to be 0.07 and 0.04 ppm, respectively [3]. As a result, the development of a simple method, coupled with real-time detection and portability for instantaneously reporting the results of nickel monitoring in the environmental and industrial areas, is considerably important to diminish hospitalization and mortality incurred by human exposure to nickel.

Currently, several analytical approaches for nickel determination have been developed such as atomic absorption spectrometry [4], inductively coupled plasma mass spectrometry [5,6] and electrochemical methods [7–9]. Although all of these techniques offer highly selective, sensitive and accurate quantification of metals, they are usually high in operation cost, time-consuming, and in need of sophisticated equipments.

Recently, colorimetric assay based on metal nanoparticles has attracted increasing attention because of their simplicity, outstandingly prompt measurement, high sensitivity, and adequate miniaturization of the sensing devices. Among colorimetric sensors, silver nanoparticles (AgNPs) have been used as an alternative yet promising colorimetric sensor because it is low-priced material with higher extinction coefficients (approximately 100 fold) compared

* Corresponding author. Tel.: +662 218 7613; fax: +662 218 7598.
E-mail address: narong.pr@chula.ac.th (N. Praphairaksit).

http://dx.doi.org/10.1016/j.talanta.2014.04.085
0039-9140/© 2014 Elsevier B.V. All rights reserved.

with gold nanoparticles (AuNPs). Therefore, the use of AgNPs might lead to improve the optical sensitivity using conventional absorbance measurement [10]. Furthermore, AgNPs have various shapes such as nanospherical, nanoplate, and nanorod depending on their synthesis via the seed-mediated method and using different stabilizers [11]. Being distinguished from other AgNPs, silver nanoplates (AgNPls), which is a kind of AgNPs with platelet configuration, exhibit broader range of absorption and scattering properties in both visible and near-IR regions of the spectrum which can improve the optical properties of AgNPs and enhance its sensitivity as a sensor [12]. In general, a key conceptual development of metal nanoparticles based colorimetric assay is the modification of its surface. Ligand-modified surface of AgNPs have been increasingly explored for selective and sensitive detection of metals of interest [13–16]. Aminothiols are widely applied as ligands for such modification because sulfur-containing compounds can be easily bound onto the surface of AgNPs [17]. The addition of target metal results in the aggregation of AgNPs, followed by the changes in color and absorption spectrum [18]. For example, Ratnarathorn et al. used homocysteine (Hcy) and dithiothreitol (DTT) to modify AgNPs for detection of Cu^{2+} in water [19]. Vasimalai et al. developed a method for detection of Hg^{2+} using mercaptothiadiazole capped AgNPs [20]. Li et al. used glutathione stabilized AgNPs to selectively detect Ni^{2+} [21]. Shang et al. developed a colorimetric detection of Ni^{2+} using N-acetyl-L-cysteine-functionalized AgNPs [2]. Based on these previous approaches, the detection limit of Ni^{2+} is somewhat inadequate for certain applications. Consequently, our objective in this work is to develop a modified AgNPs sensor for a facile, selective and highly sensitive detection of Ni^{2+}.

Here, a novel colorimetric assay for Ni^{2+} detection using glutathione (GSH) and L-cysteine (Cys) modified surface of AgNPls was developed. The pink color of AgNPls changed to purple in accordance with the Ni^{2+} level added as the aggregation of AgNPls induced by Ni^{2+} leads to a decrease in the localized surface plasmon resonance absorption peak and the formation of a new red-shifted peak. Under the optimal condition, the detection limit can be obtained as low as 7.02 ppb or 120 nM ($S/N=3$). This is by far the lowest that has been reported for AgNPls-based assays of Ni^{2+}. Moreover, the present approach has been successfully applied to detect Ni^{2+} level in effluents from a jewelry factory and a car manufacturer. The findings obtained with this proposed method were then verified and found to be in good agreement with those using inductively coupled plasma optical emission spectrometry (ICP-OES).

2. Experimental

2.1. Chemicals and materials

All chemicals were of analytical grade and used without further purification. The water used throughout this experiment was purified through a Millipore system with a resistance of 18 MΩ cm^{-1}. Glutathione (GSH) and L-cysteine (Cys) were purchased from Sigma Aldrich (St. Louis, MO). A standard solution of 1000 ppm Hg(II), As(III) and Co(II) were purchased from Spectrosol (Poole, UK), and standard solutions of 1000 ppm Ni(II), Au(III), Pt (II), Rh(II), Ag(I) and Al(III) were purchased from Merck (Darmstadt, Germany), and used as the stock solution. The following chemicals were used as received: iron chloride hexahydrate ($FeCl_3 \cdot 6H_2O$), iron sulfate heptahydrate ($FeSO_4 \cdot 7H_2O$), zinc nitrate trihydrate ($(ZnNO_3)_2 \cdot 3H_2O$) and disodium hydrogen phosphate (Na_2HPO_4) (Merck, Darmstadt, Germany), copper sulfate ($CuSO_4$) (Analar, Fontenay-sous-Bois, France), cadmium sulfate ($CdSO_4$) (Baker Analyzed, Phillipsburg, NJ), lead sulfate ($PbSO_4$) (Unilab, Scoresby Vic, Australia), potassium chloride (KCl) (Univar, Redmond, WA), calcium chloride ($CaCl_2$) (Laboratory chemicals, Dawsonville, GA), magnesium sulfate ($MgSO_4$) and potassium dihydrogen phosphate (KH_2PO_4) (Sigma-Aldrich, St. Louis, MO). AgNPls were obtained from the Sensor Research Unit at the Department of Chemistry, Faculty of Science, Chulalongkorn University, Thailand.

2.2. Instrumentation

UV–visible absorption spectra were recorded by a HEWLETT PACKARD 8453 UV–visible spectrometer (Agilent Technologies, UK) using a conventional 1.0 cm quartz cell. Infrared spectra were obtained with KBr pellets on a Nicolet 6700 FTIR spectrometer (Nicolet, USA). Transmission electron microscopy (TEM) was recorded by a H-7650 transmission electron microscope (Hitachi Model, Japan). Atomic emission measurement was performed on iCAP 6500series inductively coupled plasma optical emission spectrometer (ICP-OES) (Thermo Scientific, USA). The pH of the solution was measured with S220 SevenCompact™ pH/Ion (Mettler Toledo, Switzerland). Photographs were taken with Canon EOS 1000 D1 camera (Japan).

2.3. Synthesis and modification of the AgNPls

AgNPls were synthesized by following the reported procedure using the chemical reduction process [12]. Sodium borohydride and methyl cellulose solution were used as the reducing agent and stabilizer, respectively. The actual shapes, particle, and size distributions of the AgNPls with nominal mean diameters of 30 nm were studied by TEM. For the modification step, the GSH-Cys-AgNPls solution was prepared via self-assembly of the aminothiol on the AgNPls surface. Briefly, 1000 μL of 50 μM GSH and 5000 μL of 50 μM Cys were added into 44 mL of 0.1 mM AgNPls solution and stirred for about 2 h to ensure a complete self-assembly of the GSH and Cys onto the surface of AgNPls. After that, the characterization of the unmodified and modified AgNPls were conducted using UV–vis and FTIR spectroscopy.

2.4. Colorimetric detection of Ni^{2+}

Various concentrations of Ni^{2+} were prepared using serial dilution of the stock solution by 0.05 M phosphate buffer pH 8 (KH_2PO_4 and Na_2HPO_4) to evaluate the sensitivity and linearity of the GSH-Cys-AgNPls. Colorimetric detection of Ni^{2+} solutions were performed at room temperature by mixing 1500 μL of different concentrations of Ni^{2+} and 1500 μL of the GSH-Cys-AgNPls and the AgNPls aggregation were monitored thereafter. The AgNPls aggregation with Ni^{2+} in the solution was recorded using UV–vis spectrometry at 618 nm. A calibration curve was constructed with linear least square regression analysis. The limit of detection (LOD) and the limit of quantitation (LOQ) were calculated as 3 SD_{bl}/S and 10 SD_{bl}/S, respectively, where SD_{bl} is the standard deviation of the blank measurement ($n=11$) and S is the sensitivity of the method obtained as the slope of the calibration curve.

2.5. Applications to Ni^{2+} detection in real waste samples

The proposed method was applied for Ni^{2+} determination in real waste samples. The samples were effluents obtained from a jewelry factory and a car manufacturer in the suburb of Bangkok. Prior to analysis, the sample solution was prepared by simply mixing with 0.05 M phosphate buffer pH 8. The solution was subsequently mixed with GSH-Cys-AgNPls and its absorbance was

measured at 618 nm. The Ni^{2+} in each sample was then determined and compared with those obtained from ICP-OES method.

3. Results and discussion

3.1. Characterization of GSH-Cys-AgNPls

To investigate the incorporation of GSH-Cys onto the AgNPls surface, FTIR and UV–vis spectroscopy were respectively performed. Fig. 1A shows the infrared spectra of pure GSH, pure Cys and GSH-Cys-AgNPls. The characteristic peak of –SH at 2522 and 2549 cm^{-1} in pure GSH and Cys had significantly disappeared in the FT-IR spectrum of GSH-Cys-AgNPls. The result indicated that GSH and Cys had been successfully modified onto the surface of AgNPls via the –SH group of these compounds, corresponding to similar results observed in the previous literature reports [22]. In Fig. 1B, the UV–vis spectra show that the localized surface plasmon resonance (LSPR) absorption peak of AgNPls was shifted from 487 nm to 501 nm after the addition of the GSH-Cys modifier. We believe that the red-shifted band is mainly caused by the decrease of the plasma oscillation frequency around the nanoparticles from the binding between thiol-containing compounds and the silver nanoplates [23].

3.2. Colorimetric assay of Ni^{2+}

Following the AgNPls synthesis and modification, a colorimetric analysis using GSH-Cys-AgNPls was performed for the detection of Ni^{2+}. The color and absorption spectra of the modified AgNPls solutions with and without Ni^{2+} are shown in Fig. 2A while their TEM images are displayed in Fig. 2B. The TEM image (Fig. 2B Left) clearly shows that the GSH-Cys-AgNPls was well dispersed in aqueous solution. The average size of GSH-Cys-AgNPls was estimated to be around 30 nm and the original pink color of the silver nanoplates was maintained. After the addition of Ni^{2+} (Fig. 2B Right), the GSH-Cys-AgNPls aggregation was induced by an interaction between Ni^{2+} and GSH-Cys-AgNPls, resulting in the decrease of absorption band at 501 nm and the formation of a new absorption band at 618 nm (red shift) as illustrated in Fig. 2A. Moreover, the resulting color of GSH-Cys-AgNPls solution clearly changed to purple immediately which suggested the enlargement of the nanoparticles. Ni^{2+} is known to bind easily with ligands containing lone pair electrons such as $–NH_2$ or –COOH via coordination bonds. Both of these functional groups are contained within the structure of GSH and Cys and so it was believed that Ni^{2+} can preferentially bind to these moities and possibly participate in the cross-linking between the GSH-Cys-capped AgNPls [21,24]. These binding interactions can all contribute to the aggregation mechanism of the AgNPls as schematically illustrated in Fig. S1. According to the considerable change in color and LSPR absorption of GSH-Cys-AgNPls toward the addition of Ni^{2+}, the development of a novel colorimetric GSH-Cys-AgNPls sensor for Ni^{2+} determination was successfully accomplished.

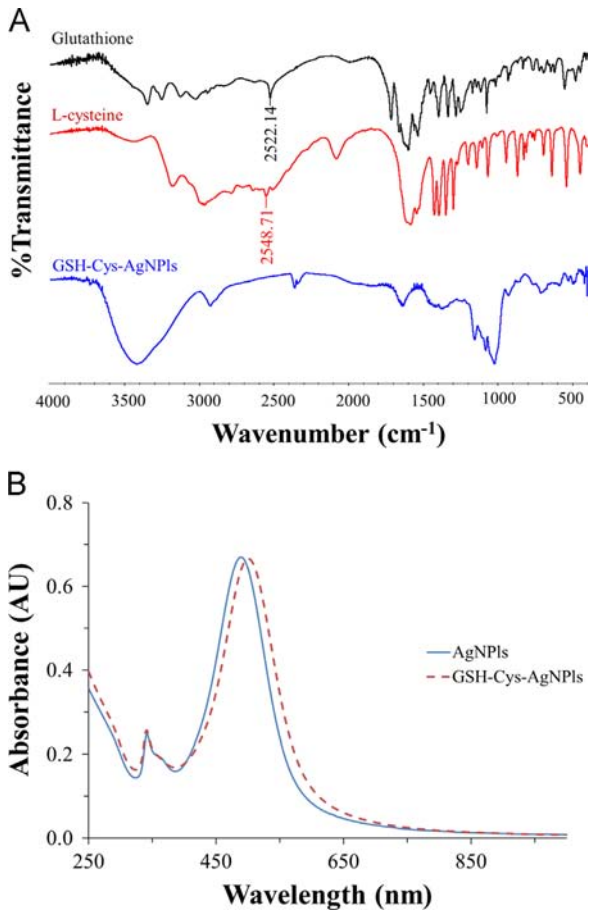

Fig. 1. (A) FT-IR spectra of pure GSH, pure Cys and GSH-Cys modified AgNPls and (B) absorption spectra of unmodified AgNPls and GSH-Cys modified AgNPls in aqueous solution.

3.3. Optimization

In this section, various optimization parameters including modifier ratio, pH, and reaction time were examined. The resulting aggregation capability between Ni^{2+} and GSH-Cys-AgNPls in each condition was observed using the absorbance measurement at 618 nm. First, the modifier concentration in different proportions (0.5–5 μM) was investigated. Interestingly, the GSH and Cys concentrations over 5 μM resulted in the self-aggregation of AgNPls without the presence of Ni^{2+} (data not shown), leading to the decrease in sensitivity of Ni^{2+} detection. In Fig. 3A, the highest absorbance at 618 nm was obtained using GSH and Cys concentration ratio of 1:5, distinguishing clearly from the other GSH and Cys proportions. We believe that this optimal GSH and Cys ratio provides greater aggregation via the interaction between Ni^{2+} and an appropriate surface modification of GSH-Cys-AgNPls, similarly to those observed for Mn^{2+} in the different works reported previously [16].

Next, the influence of pH over the range of 2.5–11.0 on the aggregation process was studied. As shown in Fig. 3B, the highest aggregation was readily attained in the vicinity of pH 7.0 and 8.0, as clearly indicated by its increasing absorbance. Although the phosphate buffer pH 7.0 provided the greatest intensity, its selectivity towards the Ni^{2+} detection was enormously decreased (Fig. S2). On the other hand, at pH 8.0, a substantial absorbance from Ni^{2+}-GSH-Cys-AgNPls was still maintained while a negligible response from other metal ions was observed. According to the pK_a of GSH and Cys [25], we believe that these functional groups on both GSH and Cys are presumably deprotonated at pH 8, creating negatively charged binding sites. The selective aggregation between Ni^{2+} and GSH-Cys-AgNPls under this condition could possibly result from the combined influences of specific size, charge, and coordination bonding of Ni^{2+} and the moieties on the AgNPls. This result suggests that GSH-Cys-AgNPls at pH 8 can be utilized to specifically detect Ni^{2+} by selective aggregation in the presence of other metal species.

Another important aspect in the aggregation between GSH-Cys-AgNPls and Ni^{2+} is the reaction time. As shown in Fig. S3, the absorbance of GSH-Cys-AgNPls after the addition of Ni^{2+} were measured at various incubation times. The result indicated that

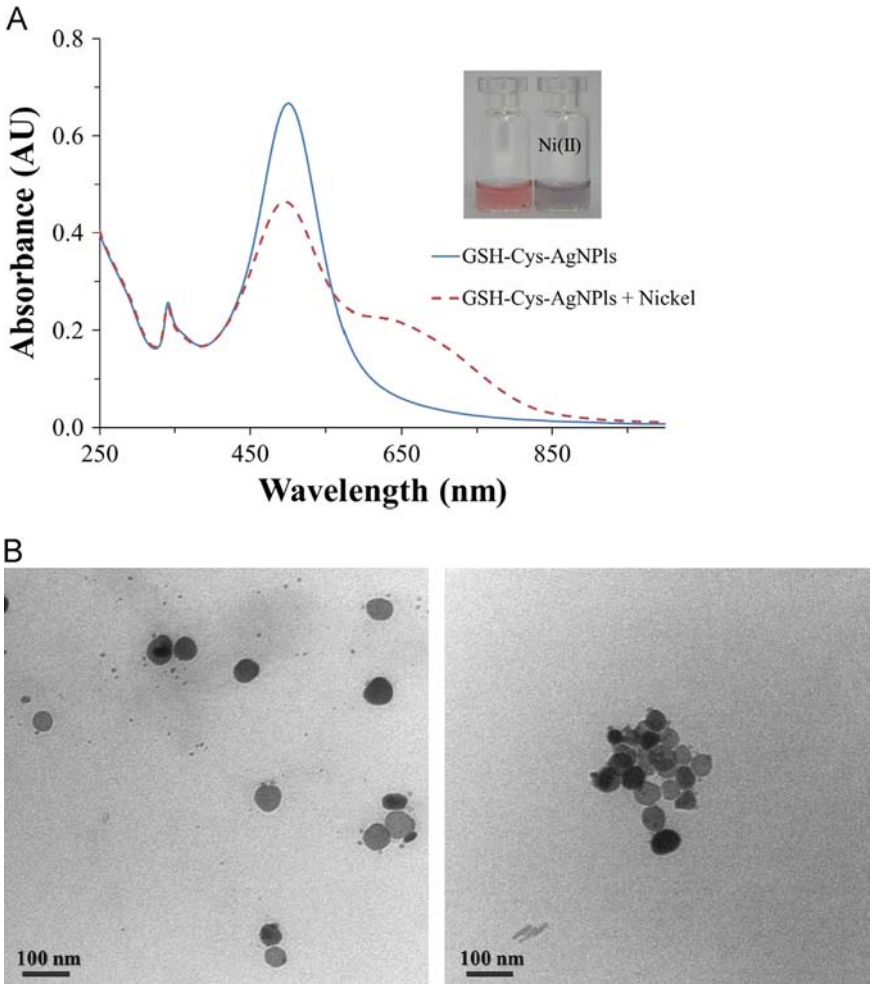

Fig. 2. (A) Absorption spectra and (B) TEM images of the dispersed GSH-Cys-AgNPls (Left) and aggregated GSH-Cys modified AgNPls induced by the addition of Ni^{2+} (Right).

the absorbance of GSH-Cys-AgNPls at 618 nm continually increased with time and became relatively steady within 6 min. Therefore, the optimal conditions consisting of GSH and Cys ratio of 1:5, phosphate buffer pH 8, and reaction time at 6 min were chosen for further experiments to provide the preferable sensitivity for Ni^{2+} detection.

3.4. Effect of interfering metal ions

To further investigate the selectivity of this method, several concentrations of other foreign metal ions including Fe^{3+}, Fe^{2+}, As^{3+}, Co^{2+}, Cu^{2+}, Cd^{2+}, Pb^{2+}, Zn^{2+}, Hg^{2+}, Au^{3+}, Rh^{2+}, Pt^{2+}, Ag^{+} (transition-metal ions), Na^{+}, K^{+} (alkali), Mg^{2+}, Ca^{2+} (alkaline earth) and Al^{3+} were studied under the optimal conditions. The UV–vis spectra and photo images of GSH-Cys-AgNPls containing Ni^{2+} along with these metals are shown in Fig. 4. The results demonstrate that only Ni^{2+} induced a remarkable aggregation of GSH-Cys-AgNPls while no significant response was observed from other metal ions. In addition, the tolerance concentration of interfering metal ions on the Ni^{2+} determination using the present colorimetric sensor is shown in Table 1. This tolerance ratio was defined as the concentration ratio of interfering metal ions that produced *a* $\pm$5% change in absorbance to that of Ni^{2+}. According to the results, it can be seen that the interferences from almost all metal ions studied did not affect Ni^{2+} detection. Nevertheless, only Pt^{2+} probably impacted the reliability and sensitivity of the proposed colorimetric sensor and thus needed to be removed, masked or even diluted to a level that no longer influenced the analytical findings.

3.5. Detection range and method detection limit

Fig. 5 shows UV–vis spectra of GSH-Cys-AgNPls solution with added various concentrations of Ni^{2+} at incubation time of 6 min. With the increase of Ni^{2+} concentration, the absorbance of GSH-Cys-AgNPls at 501 nm was significantly reduced while an absorption peak of aggregated Ni^{2+}-GSH-Cys-AgNPls at 618 nm was dramatically increased. A linear relationship between the absorbance at 618 nm and Ni^{2+} concentration in the calibration curve was established. A good linearity was observed for the concentration of Ni^{2+} ranging from 10 ppb to 150 ppb with a correlation coefficient of 0.9971. The limit of detection and the limit of quantitation for Ni^{2+} ions were found to be 7.02 ppb ($S/N=3$) and 23.01 ppb ($S/N=10$), respectively. The performance of the colorimetric GSH-Cys-AgNPls sensor was compared to the other colorimetric nanoparticle sensor used for the Ni^{2+} detection as shown in Table S1. It is clearly seen that the developed GSH-Cys-AgNPls sensor shows a relatively higher colorimetric sensitivity and lower LOD for Ni^{2+} detection.

3.6. Analysis of real samples

To evaluate the efficiency of our method, the colorimetric sensor was used to detect Ni^{2+} in waste samples from a jewelry

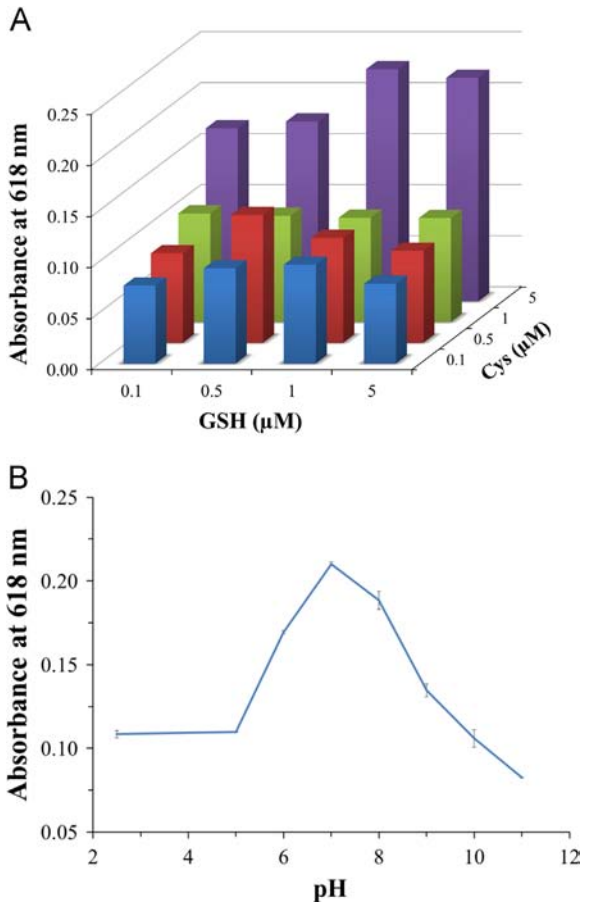

Fig. 3. (A) Effect of GSH and Cys ratio on the modification of AgNPls for the detection of Ni^{2+} using absorbance at 618 nm and (B) absorbance at 618 nm of GSH-Cys–AgNPls solutions with different pH ranging from 2.5 to 11.0 when adding Ni^{2+} solution.

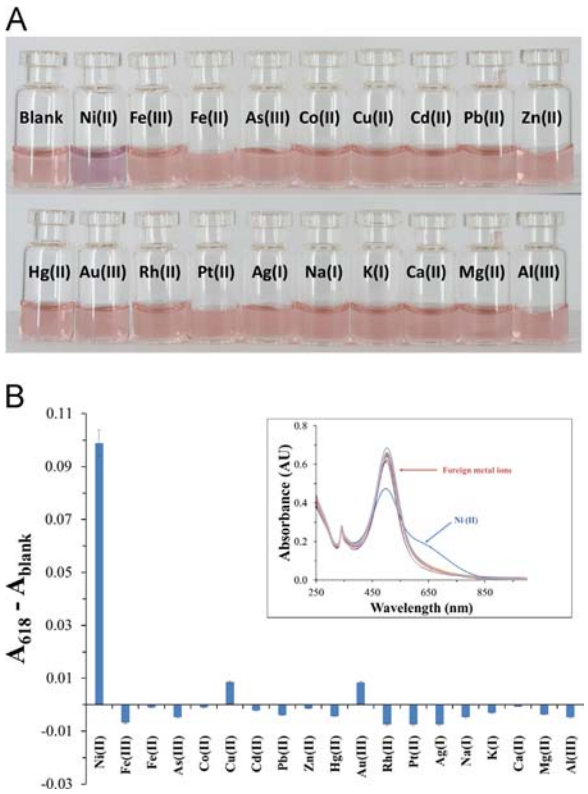

Fig. 4. (A) Photographs and (B) absorbance of GSH-Cys modified AgNPls in the presence of Ni^{2+} (70 ppb) and other foreign metals (70 ppb) including Fe^{2+}, Fe^{3+}, As^{3+}, Co^{2+}, Cu^{2+}, Cd^{2+}, Pb^{2+}, Zn^{2+}, Hg^{2+}, Au^{3+}, Rh^{2+}, Pt^{2+}, Ag^{+}, Na^{+}, K^{+}, Ca^{2+}, Mg^{2+}, Al^{3+} and (inset) UV–vis spectra of GSH-Cys-AgNPls containing various metal ions.

factory and a car manufacturer, and the results were compared with ICP-OES as shown in Table 2. Despite a number of co-existing matrix elements in these wastes, i.e., Au^{3+}, Ag^{+}, Cu^{2+}, Zn^{2+}, Cd^{2+}, Co^{2+}, etc., in the jewelry effluent and Fe^{2+}, Al^{3+}, Cu^{2+}, Pb^{2+}, Zn^{2+}, K^{+}, Mg^{2+}, Co^{2+}, etc., in the car manufacturer effluent, the Ni^{2+} findings for both samples were in good agreement with the values obtained from ICP-OES. Therefore, it was clearly demonstrated that this proposed colorimetric sensor can be applied for the selective Ni^{2+} determination of real waste samples with satisfactory results.

4. Conclusion

In summary, a novel colorimetric sensor using GSH-Cys modified AgNPls was successfully developed and applied for the selective determination of nickel ions. Under the optimum conditions, the functionalized colorimetric platform for the selective detection of trace Ni^{2+} shows superb sensitivity and selectivity towards the nickel detection in the presence of other interfering metal ions. Finally, the procedure has been successfully used to determine Ni^{2+} in waste samples from a jewelry factory and a car manufacturer with good agreement to those obtained from the standard ICP-OES method. As a result, this present method provides a simple, rapid, and cost-effective sensing of nickel ion for practical applications.

Table 1
Tolerance ratios of interfering ions in the determination of Ni^{2+} (70 ppb).

Interferences	Tolerance ratio ($C_{ions}/C^{2}_{Ni}{}^{+}$)
Rh^{2+}, Ag^{+}, Ca^{2+}, Al^{3+}	64
Zn^{2+}, Fe^{3+}, Mg^{2+}, K^{+}	16
Hg^{2+}, Na^{+}	8
Cu^{2+}, Fe^{2+}, Au^{3+}, Co^{2+}, As^{3+}, Cd^{2+}, Pb^{2+}	4
Pt^{2+}	2

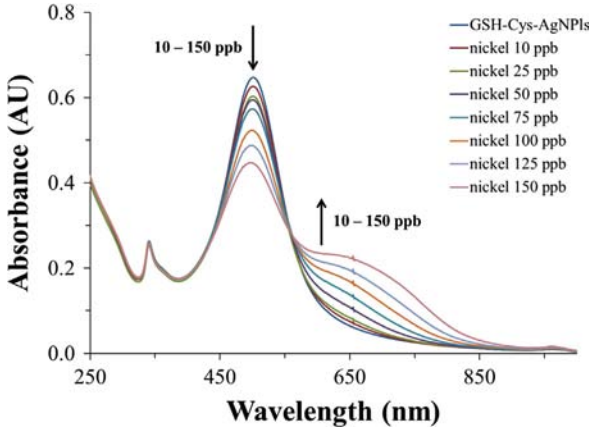

Fig. 5. The UV–vis spectra of GSH-Cys-AgNPls solutions with various concentrations of Ni^{2+} ranging from 10 to 150 ppb with incubation time of 6 min.

Table 2
Ni^{2+} determination of waste samples using the developed method and the conventional ICP-OES method ($n=3$).

Source of effluents	Our method (mean ± SD); ppb	%RSD	ICP-OES (mean ± SD); ppb	%RSD
Jewelry factory	53.72 ± 1.18	2.20	51.63 ± 0.01	1.56
Car manufacturer	65.94 ± 2.46	3.67	63.53 ± 0.07	1.17

Acknowledgments

This work was supported by the Center of Excellence on Petrochemical and Materials Technology and the Electrochemistry and Optical Spectroscopy Research Unit, Chulalongkorn University, and Grants from the Thailand Research Fund. We would also like to thank Assoc. Prof. Dr. Sanong Ekgasit, Sensor Research Unit at the Department of Chemistry, Chulalongkorn University, for the synthesis of AgNPls. The inductively coupled plasma optical emission spectrometer was provided courtesy of Sci Spec Co., Ltd. (ThermoScientific, iCAP 6500).

Appendix A. Supplementary material

Supplementary data associated with this article can be found in the online version at http://dx.doi.org/10.1016/j.talanta.2014.04.085.

References

[1] J.L. Gerding, Toxicological Profile for Nickel, 2004.
[2] Y. Shang, F. Wu, L. Qi, J. Nanopart. Res. 14 (2012).
[3] G. Aragay, J. Pons, A. Merkoçi, Chem. Rev. 111 (2011) 3433–3458.
[4] Z. Bahadir, D. Ozdes, V.N. Bulut, C. Duran, H. Elvan, H. Bektas, M. Soylak, Toxicol. Environ. Chem. 95 (2013) 737–746.
[5] D. Ying-Qiu, Y. Yi-Dong, F. Nai-Ying, C. Peng-Gang, Z. Xiao-Bo, J. Hai-Tao, S. Hong, Q. Qiu-Yao, S. Zhi-Bo, C. Yue-Xin, Chin. J. Anal. Chem. 40 (2012) 1890–1896.
[6] N. Xi-du, L. Yi-zeng, T. You-gen, X. Hua-lin, J. Cent. South Univ. 19 (2012) 2416–2420.
[7] S. Neodo, M. Nie, J.A. Wharton, K.R. Stokes, Electrochim. Acta 88 (2013) 718–724.
[8] T. Nurak, N. Praphairaksit, O. Chailapakul, Talanta 114 (2013) 291–296.
[9] R. Segura, M. Pradena, D. Pinto, F. Godoy, E. Nagles, V. Arancibia, Talanta 85 (2011) 2316–2319.
[10] W. Leesutthiphonchai, W. Dungchai, W. Siangproh, N. Ngamrojnavanich, O. Chailapakul, Talanta 85 (2011) 870–876.
[11] H.K. Sung, S.Y. Oh, C. Park, Y. Kim, Langmuir 29 (2013) 8978–8982.
[12] T. Parnklang, C. Lertvachirapaiboon, P. Pienpinijtham, K. Wongravee, C. Thammacharoen, S. Ekgasit, RSC Adv. 3 (2013) 12886–12894.
[13] D.R. Bae, W.S. Han, J.M. Lim, S. Kang, J.Y. Lee, D. Kang, J.H. Jung, Langmuir 26 (2010) 2181–2185.
[14] Z. Cui, C. Han, H. Li, Analyst 136 (2011) 1351–1356.
[15] Y. Lin, C. Chen, C. Wang, F. Pu, J. Ren, X. Qu, Chem. Commun. 47 (2011) 1181–1183.
[16] Y. Zhou, H. Zhao, C. Li, P. He, W. Peng, L. Yuan, L. Zeng, Y. He, Talanta 97 (2012) 331–335.
[17] Y. Xue, H. Zhao, Z. Wu, X. Li, Y. He, Z. Yuan, Analyst 136 (2011) 3725–3730.
[18] L. Qi, Y. Shang, F. Wu, Microchim. Acta 178 (2012) 221–227.
[19] N. Ratnarathorn, O. Chailapakul, C.S. Henry, W. Dungchai, Talanta 99 (2012) 552–557.
[20] N. Vasimalai, G. Sheeba, S.A. John, J. Hazard. Mater. 213–214 (2012) 193–199.
[21] H. Li, Z. Cui, C. Han, Sens. Actuators B: Chem. 143 (2009) 87–92.
[22] P. Sudeep, S. Joseph, K. Thomas, J. Am. Chem. Soc. 127 (2005) 6516–6517.
[23] H. Li, F. Li, C. Han, Z. Cui, G. Xie, A. Zhang, Sens. Actuators B: Chem. 145 (2010) 194–199.
[24] C.S. Keskin, S.Y. Keskin, A. Özdemir, Rev. Chim. 63 (2012) 598–602.
[25] J.T. Edsall, J. Wyman, Biophys. Chem. (1958) 1902–2002.